Marginal Nature of DNA Solutions

Eyal Shafran,[1] Alon Yaniv,[1] and Oleg Krichevsky[1,2,*]

[1]*Physics Department, Ben-Gurion University, Beer-Sheva 84105, Israel*

[2]*Ilse Kats Center for Nanoscience, Ben-Gurion University, Beer-Sheva 84105, Israel*

(Received 11 January 2010; published 23 March 2010)

We adapt a scanning fluorescence correlation spectroscopy technique to measure the structure factor of complex fluid systems and present the first measurements of the structure of semidilute solutions of long DNA polymers. The measured structure factors exhibit screening effects which, as expected for semidilute polymer solutions, grow stronger with increasing DNA concentration c. The measured concentration dependence of the screening length $\xi \propto c^{0.53\pm0.02}$ is unusual, but can be understood within the framework of a marginal solutions theory for semiflexible polymers.

DOI: 10.1103/PhysRevLett.104.128101 PACS numbers: 87.14.gk, 87.15.N−, 87.80.Nj

In polymer physics we distinguish dilute solutions, in which interactions between different chains are rare and correlations in monomer positions, characterized by the correlation function $g(r) = \langle \delta c(0) \delta c(r) \rangle$ of monomer density c, extend over a size of a polymer coil. At concentrations above polymer overlap concentration c^*, the polymer solution is in a semidilute regime, where collisions between segments of different chains shield the interactions between same chain monomers. Using a mean-field approach Edwards showed [1] that this leads to the screening of correlations in monomer positions with characteristic length scaling as $\xi \propto c^{-1/2}$. de Gennes and co-workers [2,3] argued that for flexible polymers, the mean-field theory gives incorrect $\xi(c)$ dependences, and scaling arguments should be applied instead. These predict $\xi \propto c^{-3/4}$ in good solvents (in which monomer interactions are repulsive) and $\xi \propto c^{-1}$ in theta solvents (in which attraction between monomers balances out their repulsive interactions). The predictions for these two cases are supported by experiments [3–5].

The situation differs for semiflexible polymers even though for contour lengths L and at spatial scales larger than their persistence length L_p they appear as flexible. Because of their large L_p, semiflexible coils occupy relatively large volumes as compared to flexible chains of the same length. The collisions between monomers in such coils are rare and the effects of excluded volume interactions are relatively weak. Yet, the excluded volume itself is larger than zero. These conditions were termed *marginal* by Schaeffer, Joanny, and Pincus (SJP) who predicted a wide variety of different regimes in such solutions [6]. In particular, SJP argue that because of the weakness of the excluded volume interactions in marginal solutions, the mean-field approach can be applied, and the Edwards description of screening with $\xi \propto c^{-1/2}$ should hold over a wide range of concentrations in semidilute solutions of long ($L \gg L_p$) semiflexible polymers. Remarkably, although marginal solutions are intermediate between good and theta solutions, the concentration dependence of ξ in marginal solutions is predicted to be weaker than in both of the other cases. In practice, the existence of this generic regime remains rather controversial. Some groups find $\xi \propto c^{-1/2}$ type of scaling, while others do not [5–9]. All of these measurements were carried out on synthetic polymers which have relatively small L_p and therefore, possibly, a very short range of marginal behavior.

DNA, which has a large persistence length $L_p \approx 50$ nm, should be an excellent model system to probe marginal solutions theory. Indeed, the screening length in λ-DNA solutions has been assessed indirectly through the measurements of the range of depletion interactions between two colloidal particles resulting from the presence of DNA [10,11]. The results are consistent with SJP predictions. However, although there have been several studies of dense solutions of rodlike DNA molecules [12], the structures of semidilute solutions of long DNA polymers (with $L \gg L_p$) have never been probed directly. Static light scattering has been applied to study the structure of dilute solutions of long DNA, but even in this case, it has been an experimental challenge because of strong scattering by dust particles [17].

Here we develop a new approach based on scanning fluorescence correlation spectroscopy (SFCS) [18–24], which we adapt to structural measurements by introducing a particular scanning pattern and an appropriate formalism. The simplest way to understand our approach is to imagine that DNA molecules are labeled uniformly along their contour with fluorescent dyes and are ''frozen'' in space. When such a sample is moved with a constant velocity $\vec{v}$ through a confocal excitation volume, the inhomogeneous spatial distribution of fluorophores results in fluctuations $\delta I_{\mathrm{em}}(t) = I_{\mathrm{em}} - \langle I_{\mathrm{em}} \rangle$ in fluorescence emission I_{em}. Then, the temporal correlation function $G(t) = \langle \delta I_{\mathrm{em}}(0) \delta I_{\mathrm{em}}(t) \rangle$ of fluorescence fluctuations reflects the spatial correlations $g(R)$ in fluorophore positions with $R = vt$ providing the conversion from temporal to spatial scale. Because of the final dimensions of the sampling volume, the measured correlation function $G(R)$ is, in fact, a convolution of a

characteristic excitation-emission profile and of $g(R)$, which makes it a "smeared" version of the latter. In Fourier space the spatial correlations can be deconvoluted from the sampling volume characteristics, leading to the Fourier transform of $g(R)$, which is essentially the structure factor $S(q)$ of the labeled DNA. In this Letter, we will focus on the q dependence of the structure factor and thus we will normalize its amplitude according to $S(q \to 0) = 1$.

Formally, $G(t)$ can be written as follows [25]:

$$G(t) \propto \int d\vec{r} d\vec{r}' I(\vec{r}) I(\vec{r}') \langle \delta c(\vec{r}, 0) \delta c(\vec{r}', t) \rangle \propto \propto \int d\vec{q} |\tilde{I}(\vec{q})|^2 \langle \delta \tilde{c}^*(\vec{q}, 0) \delta \tilde{c}(\vec{q}, t) \rangle, \quad (1)$$

where $\delta c(\vec{r}, t) = c(\vec{r}, t) - \langle c \rangle$ describes fluctuations in concentration of labeled DNA segments, $I(\vec{r})$ is the setup excitation-detection profile, and "tilde" denotes spatial Fourier transforms of the corresponding quantities. If DNA are "frozen," then the only changes in the spatial distribution of labels arise from the sample motion through the beam: $\delta c(\vec{r}, t) = \delta c(\vec{r} - \vec{v}t, 0)$, and hence $\delta \tilde{c}(\vec{q}, t) = \delta \tilde{c}(\vec{q}, 0) e^{i\vec{q}\,\vec{v}\,t}$. Substituting this into Eq. (1) and changing variables $\vec{R} = \vec{v}t$, we obtain

$$\tilde{G}(\vec{q}) \propto \langle |\delta \tilde{c}(\vec{q}, 0)|^2 \rangle |\tilde{I}(\vec{q})|^2 \propto S(\vec{q}) |\tilde{I}(\vec{q})|^2, \quad (2)$$

where we use the fact that for strongly labeled DNA the correlations in dye positions $\langle |\delta \tilde{c}(\vec{q}, 0)|^2 \rangle|$ reflect the structure factor $S(q)$ of DNA polymers [26]. Thus, having calibrated the instrumental characteristic $|\tilde{I}(\vec{q})|^2$ we can determine $S(q)$ from the Fourier transform of the measured SFCS functions $G(\vec{R})$ by means of Eq. (2).

In practice, the demand for the sample to be frozen in space is not strict. It is sufficient to scan the sample fast enough so that a part of the system passing through the confocal volume does not manage to change its state significantly while illuminated. We move the sample at $\sim$4 mm/s, which is the maximal speed in our setup, but similar results were obtained even with speeds as low as 1 mm/s. We also found the effects of spontaneous DNA motion on the SFCS results to be negligible for speeds above $\sim$1 mm/s by simulating SFCS data using a theory of semiflexible polymer dynamics [27]. Next, although the formalism strictly applies to a constant velocity scan along a straight line, this condition can be relaxed to a constant speed scan along any trajectory whose curvature radius at any point is much larger than the confocal volume size (≈ 0.25 μm). We scan the sample in a lateral plane along a path which can be pictured as an imperfect circle of 30 μm radius whose center orbits along another circle of 20 μm radius. Thus, the scan covers a large surface preventing frequent revisiting of same positions and associated photobleaching and correlated noise.

The measurements are performed in a homebuilt confocal setup: 514 nm line (~ 2 μW power before microscope objective) of an Ar-ion laser is deflected by a dicroic beam splitter (Q525, Chroma) into a high-power objective lens (UPLAPO 60X1.2W, Olympus). The emission is collected by the same objective, directed through a bandpass filter (HQ565/80, Chroma) into a multimode optical fiber (50 μm core) and is monitored by a fiber-coupled photon counting avalanche photodiode (SPCM-AQR-15-FC PerkinElmer) whose output is fed into a digital correlator Flex2k-12Dx2 (Correlator.com). The sample is driven by a flexure XYZ piezostage (Tritor 101, PiezoSystem Jena) equipped with capacitive sensors allowing for precise monitoring of stage position and speed. The analog voltages controlling the stage motion and monitoring stage positions were supplied by the data acquisition (DAQ) board. The DAQ board also measured the output of the position sensors. The stage was fed an analog signal pattern which was specifically optimized to keep the speed constant to within 1%–2% (standard deviation).

For all measurements presented here, we used solutions of λ-DNA [48 600 bp (base pairs)] labeled with EtBr in 10 mM phosphate pH 7.4 buffer with 137 mM NaCl, 2.7 mM KCl (PBS). Data in [28] were used to calculate dye quantities in order to keep bound dye per bp ratio constant at 1:5 for each DNA concentration. In this dye: bp ratio range, DNA properties are rather insensitive to the exact values of the ratio; such labeling does not change DNA persistence length, although it extends DNA contour length by $\sim$1.4 factor to $L \approx 22$ μm [28].

Typical SFCS correlation functions obtained from solutions of λ-DNA in 2–350 μg/mL concentration range are presented in Fig. 1 versus R^2. The screening effect can be clearly observed: the correlation functions decay at shorter distances with increasing concentration. At low concentrations the correlation curves nearly coincide, as expected for dilute polymer solutions.

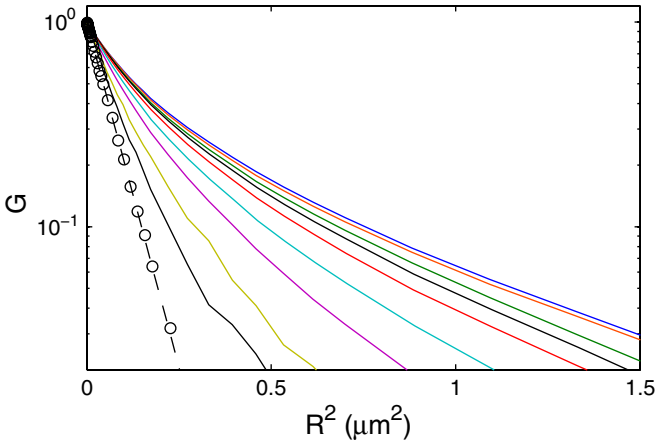

FIG. 1 (color online). Normalized to 1 SFCS correlation functions obtained from solutions of different λ-DNA concentrations (solid lines, right to left): 2.1, 5.5, 7.8, 14, 24, 47, 71, 217, and 354 μg/mL versus displacement $R = vt$. Circles with a dashed line represent the calibration of the excitation-emission profile of the optical setup. The circles are SFCS measurements of Rh6G fluorophores treated according to the left-hand side of Eq. (6) and the dashed line is a Gaussian fit to the data.

In order to extract $S(q)$ from Eq. (2), we make a standard assumption of a Gaussian confocal excitation-detection profile [29]:

$$I(\vec{r}) = I_0 \exp\left(-\frac{2(x^2+y^2)}{w_{xy}^2} - \frac{2z^2}{\omega^2 w_{xy}^2}\right), \quad (3)$$

where w_{xy} defines the width of the profile in the lateral XY plane and ω is the aspect ratio of extent of the profile in axial (Z) and lateral directions. We calibrate ω by fitting static FCS correlation curves obtained from solutions of diffusing small fluorescent carboxyrhodamine 6G (Rh6G) molecules with [29]

$$G_0^{\text{diff}}(t) = A\left(1+\frac{t}{\tau}\right)^{-1}\left(1+\frac{t}{\omega^2\tau}\right)^{-1/2}, \quad (4)$$

where τ is the characteristic diffusion time across the sampling volume and A is the correlation function amplitude. Typically, $\omega^2 \approx 30$. We deduce w_{xy} from comparison of the correlation functions obtained from diffusing dye molecules in static and scanning FCS modes. Since our pattern of scanning is equivalent to linear constant speed motion of the sample, the correlation functions $G_v^{\text{diff}}(t)$ in the scanning mode satisfy [19]

$$G_v^{\text{diff}}(t) = G_0^{\text{diff}}(t)\exp\left(-\frac{(vt)^2}{w_{xy}^2(1+t/\tau)}\right). \quad (5)$$

From the comparison of Eqs. (4) and (5) one can see that for $t \ll \omega^2\tau$

$$\left[\frac{G_v^{\text{diff}}(t)}{G_0^{\text{diff}}(t)}\right]^{A/G_0^{\text{diff}}(t)} = \exp\left(-\frac{(vt)^2}{w_{xy}^2}\right). \quad (6)$$

Indeed, the plot of the experimentally measured left-hand side of Eq. (6) versus $R^2 = (vt)^2$ is almost a perfect Gaussian with $w_{xy} \approx 0.25$ μm (Fig. 1). Direct mapping of the sampling volume by scanning fluorescent 50 nm beads gives similar values of w_{xy}. However, directly measured $I(\vec{r})$ is too noisy to extract $\tilde{I}(\vec{q})$ reliably.

Because of the spherical symmetry of $S(\vec{q})$, it is enough to perform scans in the lateral plane only in order to determine $G(\vec{q})$ and solve Eq. (2). To a very good approximation, $S(\vec{q})$ can be obtained by assuming $\omega^2 \to \infty$, in which case $|\tilde{I}(\vec{q})|^2$ and $\tilde{G}(\vec{q})|$ are nonzero in lateral directions only. Then, $\tilde{G}(q)$ can be obtained from the measured $G(R)$ by means of Fourier-Bessel transform and $S(q) \propto \tilde{G}(q)\exp(w_{xy}^2 q^2/4)$. This result serves as a starting point in an iterative procedure which takes into account final ω^2. At each iteration the expected $G(R)$ is calculated from $I(\vec{r})$ and from $S(q)$ obtained at the previous iteration, and the difference between the expected and measured $G(R)$ is used to obtain corrections for $S(q)$. The starting approximation is, in fact, so good that it is enough to perform one-step iteration to bring about convergence.

The normalized to unity structure factors obtained from the measured $G(R)$ are presented in Fig. 2. At the lowest

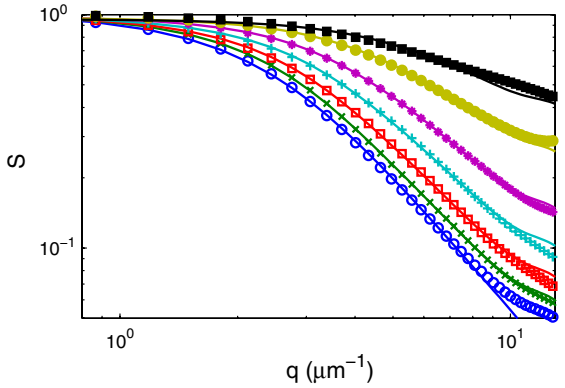

FIG. 2 (color online). Symbols represent measured structure factors $S(q)$ for solutions of different DNA concentrations (left to right): 2.1, 7.8, 24, 47, 71, 217, and 354 μg/mL. The leftmost line is fit to $S(q)$ of dilute solution ($c = 2.1$ μg/mL) with Debye expression Eq. (7). Other lines are fits to the data in semidilute regime using Eq. (8).

measured concentrations $c < 4$ μg/mL the structure factors can be fit very well (Fig. 2) with the Debye expression for ideal polymers:

$$S_0(q) = \frac{2}{(qR_g)^4}(e^{-q^2R_g^2} - 1 + q^2R_g^2), \quad (7)$$

giving the gyration radius of DNA coil $R_g = 0.64 \pm 0.02$ μm. The quality of the fit is remarkable and points to the weak excluded volume effects as expected for DNA coils [30]. The R_g value itself points to ~5% expansion with respect to the size of an ideal semiflexible chain of 22 μm contour length and $L_p = 50$ nm. For unperturbed λ-DNA with $R_g \approx 0.5$ μm, the overlap concentration of $c^* \approx 20$–30 μg/mL has been measured [10,31]. Since $c^* \propto M/R_g^3$ (where M is polymer molecular weight), for our samples we expect $c^* \approx 10$–15 μg/mL. Indeed SFCS correlation functions start to change their shape appreciably in this range of concentrations (Fig. 1).

In order to extract the screening length ξ, we fit $S(q)$ with the expression [6]

$$S(q) = B\left(1+\frac{2\xi^2}{R_g^2 S_0(q)}\right)^{-1}, \quad (8)$$

where $S_0(q)$ and R_g are, respectively, the structure factor and gyration radius of DNA in dilute solutions, and B and ξ are the fitting parameters. As $S_0(q)$ we used the structure factor measured at $c < 4$ μg/mL, which was normalized to unity for $q \to 0$ and the corresponding R_g. The fits are presented in Fig. 2 together with the data, and the obtained dependence of ξ on base pair concentration c is shown in Fig. 3.

The best power law fit to the concentration dependence of ξ gives $\xi \propto c^{0.53\pm0.02}$, which is close to Edwards' and SJP's predictions. Furthermore, ξ^{-2} vs c dependence is close to linear (Fig. 3, inset), and from its slope the effective hard-core diameter d of DNA can be estimated.

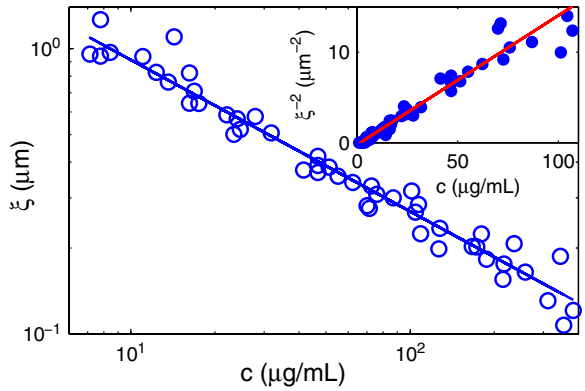

FIG. 3 (color online). Concentration dependence of the screening length ξ. Symbols are data points, solid line is the best power law fit $\xi \propto c^{0.53}$. Inset: Same data plotted as ξ^{-2} vs c. Line is the best linear fit to the data. From its slope the effective hard-core diameter of DNA is estimated to be ~4 nm.

Following SJP theory [6] (and correcting for the missing factors): $\xi^{-2} = 3\pi dc/(2n)$, where c is DNA concentration expressed as a number of base pairs per unit volume and n is the number of base pairs in a segment of length L_p ($n \approx 105$ for DNA extended by 1.4 factor). From the slope of the line in the inset of Fig. 3 we estimate $d = 3.5 \pm 0.2$ nm. This number appears reasonable as it roughly corresponds to the diameter of DNA double helix (2 nm) taken together with the associated Debye-Huckel layer (2×0.8 nm in PBS buffer).

To conclude, we develop a new approach to measure the structure of DNA solutions based on fluorescent labeling and SFCS and present the first measurements of structure factors of semidilute solutions of long DNA polymers. We observe screening effects with the characteristic length scaling as $\xi \propto c^{0.53\pm0.02}$ with DNA concentration consistent with Edwards' theory of polymer screening and with SJP's theory of marginal solutions. We note that although in this work we used only the random labeling of DNA, it is in combination with specific fluorescent labeling that our experimental approach has the greatest promise and could, in principle, assess many interesting structural features of DNA and other polymer solutions.

This work has been supported by Israel Science Foundation Grants No. 663/04 and No. 984/09.

*okrichev@bgu.ac.il

[1] S. Edwards, Proc. Phys. Soc. London **88**, 265 (1966).
[2] P.-G. deGennes, *Scaling Concepts in Polymer Physics* (Cornell University Press, Ithaca, NY, 1979).
[3] M. Daoud, J. P. Cotton, B. Farnoux, G. Jannink, G. Sarma, H. Benoit, R. Duplessix, C. Picot, and P.-G. deGennes, Macromolecules **8**, 804 (1975).
[4] T. Nicolai and W. Brown, Macromolecules **23**, 3150 (1990).
[5] W. Brown and T. Nicolai, Colloid Polym. Sci. **268**, 977 (1990).
[6] D. W. Schaefer, J. F. Joanny, and P. Pincus, Macromolecules **13**, 1280 (1980).
[7] P. Wiltzius, H. R. Haller, D. S. Cannell, and D. W. Schaefer, Phys. Rev. Lett. **51**, 1183 (1983).
[8] A. Bennett, P. J. Daivis, R. Shanks, and R. Knott, Polymer **45**, 8531 (2004).
[9] T. Uematsu, C. Svanberg, M. Nydén, and P. Jacobsson, Phys. Rev. E **68**, 051803 (2003).
[10] R. Verma, J. C. Crocker, T. C. Lubensky, and A. G. Yodh, Phys. Rev. Lett. **81**, 4004 (1998).
[11] R. Verma, J. C. Crocker, T. C. Lubensky, and A. G. Yodh, Macromolecules **33**, 177 (2000).
[12] Several studies [13–16] focused on polyelectrolyte properties of DNA, measuring structures of dense solutions of short ($L \sim L_p$) DNA molecules at low or zero salt concentrations. Interestingly, in conditions of electrolyte strength controlled by DNA counterions, one finds $\xi \propto c^{-1/2}$, although the nature of this regime is very different from that addressed here and is related to adaptation of DNA blobs shape to changes in electrostatic screening with changing DNA concentration. Here we study a more conventional polymer physics problem: $L \gg L_p$ and electrostatic interactions almost totally screened by high salt concentrations.
[13] L. Wang and V. A. Bloomfield, Macromolecules **24**, 5791 (1991).
[14] P. Wissenburg, T. Odijk, P. Cirkel, and M. Mandel, Macromolecules **28**, 2315 (1995).
[15] V. Castelletto, R. Itri, L. Q. Amaral, and G. P. Spada, Macromolecules **28**, 8395 (1995).
[16] R. Borsali, H. Nguyen, and R. Pecora, Macromolecules **31**, 1548 (1998).
[17] J. A. Harpst and J. R. Dawson, Biophys. J. **55**, 1237 (1989).
[18] M. Weissman, H. Schindler, and G. Feher, Proc. Natl. Acad. Sci. U.S.A. **73**, 2776 (1976).
[19] D. Magde, W. W. Webb, and E. L. Elson, Biopolymers **17**, 361 (1978).
[20] N. O. Petersen, D. C. Johnson, and M. J. Schlesinger, Biophys. J. **49**, 817 (1986).
[21] D. E. Koppel, F. Morgan, A. E. Cowan, and J. H. Carson, Biophys. J. **66**, 502 (1994).
[22] M. A. Digman, P. Sengupta, P. W. Wiseman, C. M. Brown, A. R. Horwitz, and E. Gratton, Biophys. J. **88**, L33 (2005).
[23] Z. Petrásek and P. Schwille, Biophys. J. **94**, 1437 (2008).
[24] J. P. Skinner, Y. Chen, and J. D. Müller, Biophys. J. **89**, 1288 (2005).
[25] B. J. Bern and R. Pecora, *Dynamic Light Scattering* (Wiley, New York, 1976).
[26] T. Romantsov, I. Fishov, and O. Krichevsky, Biophys. J. **92**, 2875 (2007).
[27] L. Harnau, R. G. Winkler, and P. Reineker, J. Chem. Phys. **104**, 6355 (1996).
[28] M. S. Rocha, M. C. Ferreira, and O. N. Mesquita, J. Chem. Phys. **127**, 105108 (2007).
[29] R. Rigler, U. Mets, J. Widengren, and P. Kask, Eur. Biophys. J. **22**, 169 (1993).
[30] J. F. Marko and E. D. Siggia, Phys. Rev. E **52**, 2912 (1995).
[31] N. Pernodet and B. Tinland, Biopolymers **42**, 471 (1997).